JOURNAL OF MATERIALS SCIENCE 12 (1977) 1994–2000

Precipitation in $Cd_xHg_{1-x}Te$

C. J. GILLHAM, R. A. FARRAR
Engineering Materials Laboratories, The University, Southampton, Hants., UK

An electron microscope study has been made of the precipitation effects at the boundaries of the pseudobinary sphalerite $Cd_xHg_{1-x}Te$ phase. Te precipitation is frequently found for alloys with compositions of 51 to 53 at. % Te but rarely in the 50 at. % stoichiometric alloy. Annealing of specimens under Hg overpressure leads to the formation of a new crystalline phase, which appears to be strongly related to the ω Cd–Hg phase.

1. Introduction

In the range of composition $0.15 < x < 0.6$ the semiconducting pseudo-binary sphalerite compound $Cd_xHg_{1-x}Te$ (CMT) has an energy gap ranging from 0 to 0.8 eV. The energy gap is continuously variable with composition and may be tailored so as to provide intrinsic photon detection in the infrared range from 2 μm upward. In particular, the atmospheric transmission window in the range 8 to 14 μm (which corresponds to energy gaps which are not found in any known elemental or ordered compound) may be covered by the composition range $0.16 < x < 0.22$. As a result of this importance $Cd_xHg_{1-x}Te$ has been the subject of much research in the last 18 years. In spite of this, however, the amount of basic metallurgical and crystallographic investigation reported, has been relatively small [1–6] and confined to the establishment of an existence region, in the P–T projection, for the ternary and the parent binary compounds. The detailed crystallography within the phase and what happens at the boundaries has not been a matter of detailed study. As the current photoconductive and photovoltaic device requirements demand the production of crystals with uniform composition and structure, a study of the nature of the second phases present in the as-grown and annealed materials is essential.

2. Experimental

Samples of cadmium mercury telluride were obtained from Mullard Ltd., Southampton, and consisted of slices, approximately 1 mm thick, cut from crystal ingots of various diameters between 5 and 13 mm. The ingots were produced by two different processes; (a) the Bridgman method and (b) quenching the melt followed by a recrystallization period at a temperature just below the solidus. The starting materials were of very high purity: Cd – 6N; Hg – 6N + additional distillation; Te – 6N + 10 zone refining. The slices used in the investigation of the metal-rich side of the phase were annealed in closed ingots in the presence of excess mercury (at the same temperature) for periods of 10 to 15 days and at temperatuures between 240 and 260° C. Initial preparation of the slices consisted of lapping and polishing in a methanol–bromine mixture (volume ratio 10:1). An A.E.I.-EM6G electron microscope was used to examine the specimens in both reflection and transmission diffraction modes as well as by transmission micrography. Specimens for transmission electron diffraction (TED) study were made from slices, thinned in a mixture of methanol and bromine. Because of the high atomic number of Hg, the crystals need to be thinned to less than 1000 Å for electron transmission to be appreciable. Furthermore there are very severe handling difficulties resulting from the brittle nature of the material. As a result of these factors large areas of uniformly thin foil are rarely obtainable. The practical course is to thin specimens until multiple perforation occurs, the microscope examination being confined to the small regions around the perforation where the material is sufficiently thin. The perforated foils were supported by copper

grids in the normal manner for microscope observation.

3. Results

3.1. The tellurium-rich phase boundary

The Bridgman ingots, in this investigation, were made from Te-rich starting materials with deviations from stoichiometry of between 1 and 3 at.% Te. Uncertainties in the free space volume and in the vapour pressure of the Hg above the melt mean that the starting materials represent only a nominal composition. The Cd composition was in the range 8 to 11 at.%, corresponding to the region of narrow band gap, of interest in infrared devices.

Reflection electron diffraction (RED) pictures consistently revealed Debye–Scherrer rings, which may be indexed as normal trigonal tellurium superimposed on a spot matrix due to the normal sphalerite structure. Although rings are usually very faint this is a fairly frequent occurrence. Since the area of crystal illuminated by the electron beam, in this position of oblique incidence, is large (of the order of 1 to 5 mm^2) the pattern represents the average situation. The amount of excess Te is not especially large, particularly since the compound phase is thought to lie mainly on the Te-rich side of stoichiometry [1], so that only occasional concentrations of precipitate are likely to show up strongly in a diffraction pattern. With TED, however, the selected area of diffraction is of the order of 1 μm^2 and on this scale nonuniformity of Te concentration is more probable (in fact precipitate is sometimes found in nominally stoichiometric material and particular areas may be found with relatively high concentrations of precipitate). Such a region is shown in Fig. 1 together with the transmission diffraction pattern from about a third of the area of the micrograph (inset).

The CMT matrix pattern is a [1 2 3] (cubic) projection. The Te ring pattern consists of a

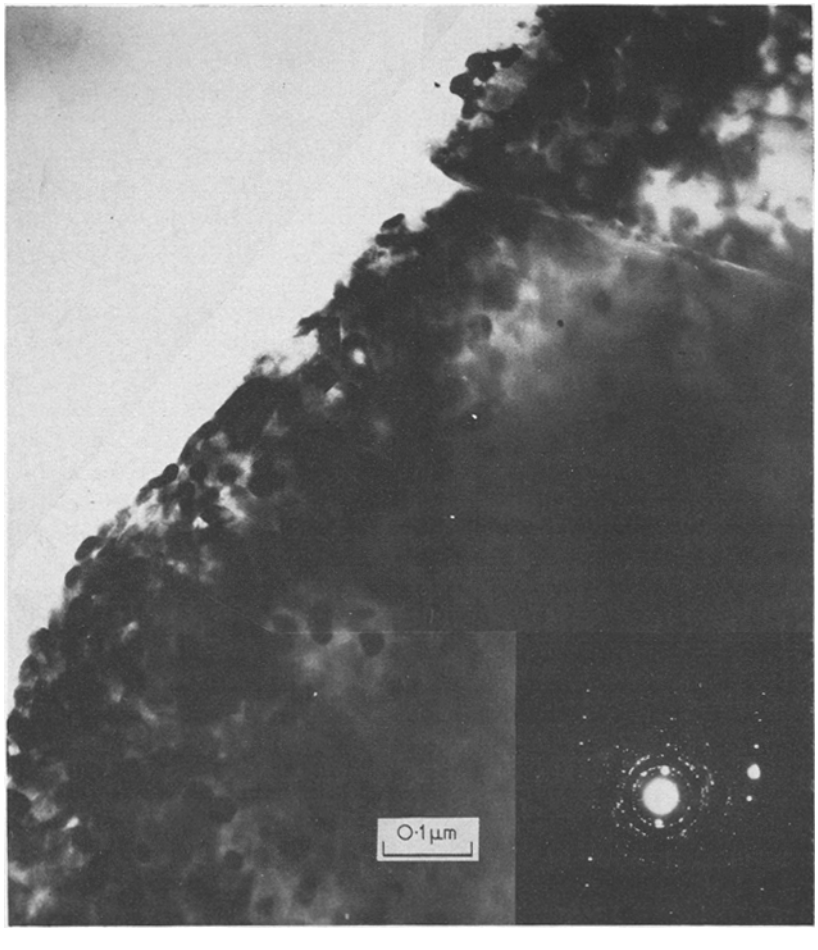

Figure 1 Electron transmission micrograph showing Te precipitation together with diffraction pattern (inset).

countable number of discrete spots. An estimate for the (1 0 0) ring is about 65 spots. By further estimating the range of incident angles for which Bragg reflection will occur (the extent of a normal single crystal pattern is a good indication) it is possible to relate these 65 spots to a total number of crystallites of between 300 and 500. For an illuminated area about 1 μm in diameter this density of crystallites corresponds, approximately, with the distribution of the roughly circular regions in the transmission micrograph in Fig. 1. The size distribution of these precipitates appears to be in the range 100 to 500 Å which is consistent with the Te spots being mostly fairly sharp. One or two of the spots are diffused to an extent suggesting crystallite sizes down to 10 Å. The general impression gained from this and other diffraction patterns is that there is no preferred orientation of the Te precipitates with respect to the CMT matrix.

Apart from sharp Te rings, diffuse ring patterns are often observed but these are usually too weak to identify. One pattern that was sufficiently strong to allow microdensitometer information to be obtained is shown in Fig. 2a, background subtracted and plotted as a function of S ($=4\pi \sin\theta/\lambda$). This specimen was from a nominally stoichiometric crystal, quenched from the melt and recrystallized at 650° C. Fig. 2b shows the equivalent plot for amorphous Te taken from Ichikawa [7]. The correlation between these patterns is surprising since Ichikawa reports that amorphous Te abruptly crystallises above 24° C, presumably irreversibly and it does not seem very likely that Te would come out of solution below this temperature. It is a possibility that amorphous Te was redeposited from the methanol–bromine etch, although an Auger spectroscopic examination of the surface condition produced by this etch did not reveal any such excess of Te [8]. In either case it is surprising that amorphous Te should survive the heating of an electron beam, which causes temperatures in excess of 24° C.

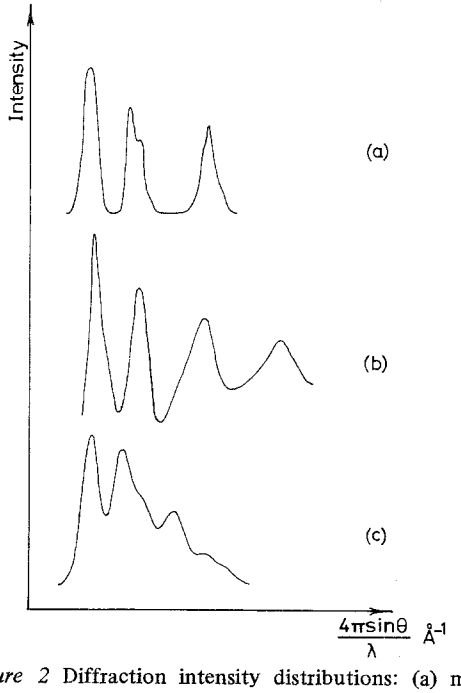

Figure 2 Diffraction intensity distributions: (a) microdensitometer plot of observed distribution, (b) amorphous Te, from Ichikawa [7], (c) theoretical distribution for (9 Å) Te microcrystals.

It was considered much more probable that the diffuse ring pattern would be generated by a distribution of small trigonal Te precipitates. Using Gaussians to represent the particle-size broadening we obtain plot Fig. 2c which represents a uniform distribution of spherical particles of Te with diameter 9 Å. While the observed pattern (Fig. 2a) reveals a tendency to shoulder on the right-hand side it, nevertheless, more nearly resembles the amorphous than the microcrystalline situation. This suggests that in the early stages of precipitation a surface energy term, due to the presence of the CMT matrix, suppresses the Ichikawa transition sufficiently to give rise to an intermediate situation between the amorphous and microcrystalline structures.

3.2. The metal-rich phase boundary

We have examined a number of CMT slices, nominally stoichiometric and annealed under excess Hg pressure. Using the methanol–bromine etch it is possible to strip successive layers, a few microns thick, from the specimen surface which is examined each time by RED. A fairly typical profiling pattern emerges. The surface which originally shows single crystal diffraction patterns, will now show a ring pattern which is sometimes slightly diffuse. This pattern is readily indexable as CMT sphalerite. This suggests either that mercury in-diffusion has destroyed the continuity of the crystal to a very considerable degree, or that a sphalerite, CMT or HgTe (RED lacks the precision to distinguish the small lattice parameter difference) layer is deposited at the surface by Te (or Te + Cd) out-diffusion. The region of polycrystallinity extends only for 1 or 2 μm. As the sphalerite pattern disappears another ring pattern emerges indicating a structure, which has never been seen

in Te-rich material, and which we will designate the ω^*-phase. Typically, this ring pattern will peak in intensity at a depth between 10 and 20 μm and thereafter tail off slowly to depths of 100 μm or more. The depth of penetration appears to increase with annealing temperature and time. When this ring pattern disappears the resulting RED pictures show the sharp single-crystal patterns of the CMT matrix.

When the d-spacings of the ω^*-phase were compared with the ASTM data file a moderately good fit was obtained with the ω-phase of the Cd–Hg binary system, although the intensities of the lines did not match up very well. The ω-CdHg phase is centred tetragonal, existing in both ordered (ω' and ω'') and disordered forms over a range of Hg compositions from 35 to 90 at.% Hg, and isostructural with the low temperature β-Hg phase [9]. The axial ratio of the body centred cell varies from 0.74 at 40 at.% Hg to 0.72 at 72 at.% Hg with β-Hg having a value 0.707.

A least squares analysis of several RED patterns gives a mean atomic volume, for the ω^*-phase, of 22.7 ± 0.8 Å^3, assuming two atoms/cell, which is consistent with the ω-Cd–Hg atomic volumes ($22.65 < \Omega < 23.16$ Å^3 for $0.72 < x_{Hg} < 1.0$ [9]. The best value for the axial ratio, however, is 0.810 ± 0.009, which is indistinguishably close to the $\sqrt{(2/3)}$ (i.e. 0.816) which would make the structure hexagonal. This curiosity revives the speculation of Mehl [10] who tried to demonstrate a connection between the ω-Cd–Hg structure and the hexagonal-close-packed Cd structure by distortions via just such a cell.

The relative intensities of the observed lines, however, are at variance with those expected from the Mehl cell, values taken from microdensitometer plots being shown in Table I. The RED intensities are the average of several plates and are compared with intensities from a transmission diffraction pattern. The patterns have exactly the same d-spacing distribution but their intensity

TABLE I

Line	Measurements			Hexagonal structures; $a = 3.118$ Å, $c = 5.401$ Å 2 atoms/cell				α-Hg (78 K)‡	
	d-spacings (Å)	intensities by microdensitometer and visual estimation		d-spacing (Å)	Intensities†			d	I
		transmission diffraction	reflection diffraction*		Mehl $u, v, w = \frac{1}{2}, \frac{1}{2}, \frac{1}{2}$	HCP $u, v, w = \frac{2}{3}, \frac{1}{3}, \frac{1}{2}$	Simple hexag. $u, v, w = 0, 0, \frac{1}{2}$		
A	2.71	31	20	2.70	133	90	160	2.74	167
B	2.37	169	40	2.42	213	186	–	2.23	133
C	1.93	156	51	1.91	67	39	120	1.73	83
D	–	–	–	1.56	22	52	40	–	–
E	1.47	30	11	1.49	164	71	–	1.46	100
F	1.35	100	100	1.35	100	100	100	1.37	100
G	–	–	–	1.31	–	55	–	–	–
H	1.19	–	17	1.21	88	31	96	1.22	17
		–	–	1.18	42	–	–	–	–
	1.11	–	25	1.08	15	37	–	1.12	83
		–	–	1.02	51	55	69	1.07	50
	1.00	–	8	1.00	61	64	–	1.00	50
	0.96	–	10 m	0.95	45	29	90	0.94	100
	0.86	–	w	0.88	61	17	13	0.91	50
	0.77	–	m	0.80	20	–	–		
	0.74	–	vw	0.74	94	–	–		
	0.67	–	vw	0.69	24	–	–		
	0.64	–	vw	0.65	24	–	–	–	–
	0.62	–	vvw	0.61	50	–	–	–	–
	0.59	–	vvvw	0.58	21	–	–	–	–
	0.52	–	vvw	0.51	44	–	–	–	–

KEY

*m = medium, vw = very weak.

†u, v, w: fractional co-ordinates of the displacement of the 2nd from the 1st atom in the hexagonal cell.

‡ASTM card 9-253.

distributions are quite different, demonstrating the difficulty in interpreting intensity information on electron diffraction plates. The RED pictures have an overall intensity distribution (governed by the absorption path factor acting against the powder-method and Lorentz factors) which peaks sharply in the region of the first few lines. The very rapid change of background in this region will therefore lead to large errors in intensity measurement. The transmission diffraction pattern, which has an overall intensity distribution that monotonically decays (probably as θ^{-2}) is more reliable. It is clear, nevertheless, that the observed intensities do not match those of the body centred hexagonal Mehl structure (shown in Table I artificially scaled by θ^{-2} and normalized to 100 at the predominant 1.35 Å line). In particular the relative intensities of lines E and F are quite different. The Mehl structure, however, probably fits the observed intensities slightly better than the hexagonal-close-packed (i.e. the Cd structure) arrangement which ought to have a medium-strong line at 1.56 Å where no line is observed at all (see Table I). The simple hexagonal variation (with the same cell and atomic volume) misses the strong observed B line entirely.

For a further comparison it is interesting to note that the observed d-spacing spectrum is also similar to that of α-Hg (at 70 K) although lines A and E are much more intense than the ω^*-lines, which always appear fainter than their immediate neighbours. The similarity of the d-spacing spectra for the Mehl structure and α-Hg appears to be coincidental. The hexagonal cell of rhombohedral Hg is quite unrelated to the Mehl cell.

It has proved extremely difficult to obtain thin foil micrographs of this new phase, as a result of beam heating. Usually the diffraction pattern from what appears to be a precipitate distribution, proves to be the diffuse ring pattern of liquid Hg [11]. In Fig. 3, however, we show a transmission micrograph of what appears to be precipitate with the hexagonal/tetragonal diffraction pattern of the ω^*-phase. The rings are on the threshold of being spotty with ~500 to 1000 spots corresponding to ~3000 to 6000 crystallites within the selected diffraction area. This appears to tally with the observed distribution on the micrograph. The precipitates which do not appear to have any preferred orientation, have diameters ~20 to 40 Å.

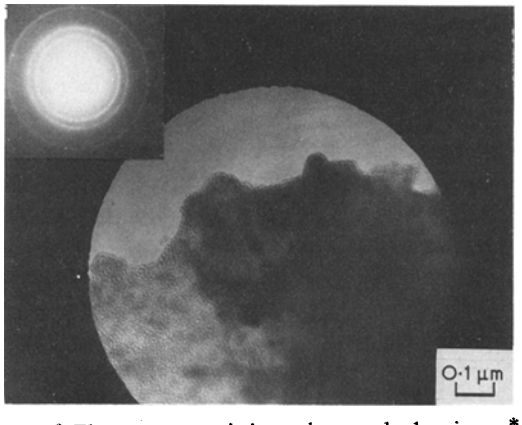

Figure 3 Electron transmission micrograph showing ω^*-phase together with diffraction pattern (inset).

4. Discussion

The existence region of the sphalerite phase is generally thought [1, 2, 4] to be mostly on the Te side of stoichiometry. While Delves and Lewis [4] give a maximum melting temperature of HgTe at 51.5 to 52 at.% Te and a phase width greater than 2 at.%, Brebrick and Strauss [1] obtain a maximum phase width of 0.6 at.% (49.9 to 50.5 at.% Te) from their optical density measurements. Bearing these results in mind, we show a schematic T–x diagram in Fig. 4.

The observation of the two forms of precipitation discussed here, appears to be consistent with such a diagram. Te precipitate is rarely seen except in material rich in Te to the extent of 1 to 3 at.%. The occasional appearance in nominally stoichiometric material is probably due to non-uniformity of composition. Whilst the possibility of Te supersaturation exists, the fact that Te precipitate is not generally observed for $x_{Te} < 0.51$, appears to reflect a compromise between the Brebrick and Strauss [1] and the Delves and Lewis [4] boundaries. On the other hand, we have observed what we have called the ω^*-phase quite often in nominally stoichiometric material (which probably means slightly Te-rich since Hg is lost in the melt stage) and very strongly after rather short Hg anneals. This suggests that the metal side of the sphalerite phase is either very close to or on the Te side of the stoichiometric line.

The present results are thus consistent with a phase width ~1 at.%, in agreement with both Delves and Lewis [4] and Brebrick and Strauss [1]. The latter authors in a further paper [12], however, fitted a simple defect model to electrical measurements and predicted a maximum phase width of 0.05 at.% Hg. We would, however, point out that the observed range of lattice parameters

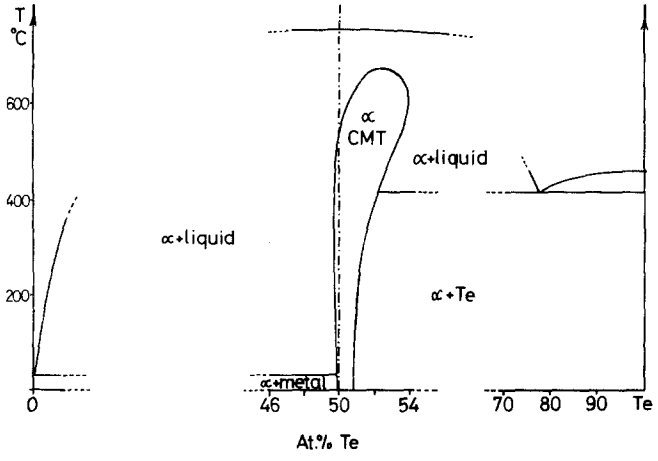

Figure 4 Schematic T–x phase diagram for $Cd_xHg_{1-x}Te$ with fixed Cd : Hg ratio.

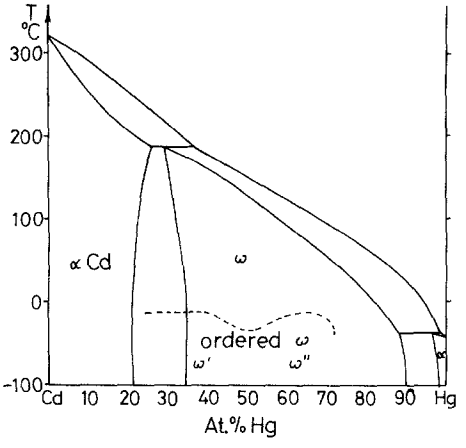

Figure 5 T–x phase diagram for the system Cd–Hg (after Claeson *et al.* [9].

for HgTe corresponds to a homogeneity range of 0.75 at.% by Vegard's Law [13]. The simple defect model would therefore seem seriously inadequate.

The exact structure of the ω^*-phase is elusive but it appears to be strongly related to the ω-phase of the Cd–Hg system. The phase diagram for this system is shown in Fig. 5. It is clear from this that for our annealing temperatures the ω-phase could not be precipitated as such, but only as the liquid Cd–Hg and furthermore, if the Cd concentration of the precipitate is less than 20 at.%, then it should remain liquid, or at least two-phase, even at room temperature. Although the observed phase is generally unstable with respect to beam heating in the thin foils it must be stable to higher temperatures than room temperature for a thin-foil diffraction pattern to have been obtained at all. It is also interesting to note that in the RED mode, where temperatures are close to room temperature, there is no evidence of liquid Hg patterns. If the phase diagram is correct this suggests either that the precipitate has a higher Cd : Hg ratio than the matrix, or that the relative energies of the liquid and solid phases are different in the sphalerite matrix, presumably affected by a strong surface energy term. There is nothing improbable in the former case, since there is no reason why the tie-line from the sphalerite phase to the metal phase, should lie in a pseudo-binary section.

The fact that the observed precipitate is solid 80 to 100° C above the normal melting point of mercury confirms that there must be a quantity of Cd in the phase. In conclusion, it is interesting to speculate that dilute Hg–Cd alloys would show some of the allotropic tendencies of pure solid Hg, which is known to exist in at least three forms [14]. Furthermore, since theoretical pseudo potential calculations indicate a large degree of instability of these forms with respect to various lattice distortions [15], it is possible that our ω^*-phase represents one such distortion.

Acknowledgements

The authors are grateful to M. Quelch and J. Harris of Mullards Ltd. (Southampton) for the provision of all the specimens. This work has been carried out with the support of Procurement Executive, Ministry of Defence sponsored by DCVD.

References

1. R. F. BREBRICK and A. J. STRAUSS, *J. Phys. Chem. Sol.* **26** (1965) 989.
2. J. L. SCHMIT and C. J. SPEERSCHNEIDER, *Infra Red Physics* 8 (1968) 247.

3. J. BLAIR and R. NEWNHAM, "Metallurgy of Elemental and Compound Semiconductors" **12** (Wiley (Interscience), New York, 1961) p. 393.
4. R. T. DELVES and B. LEWIS, *J. Phys. Chem. Sol.* **24** (1963) 549.
5. J. C. WOOLLEY and B. RAY, *ibid* **13** (1960) 151.
6. B. RAY and P. M. SPENCER, *Phys. Stat. Sol.* **22** (1967) 371.
7. T. ICHIKAWA, *ibid (b)* **56** (1973) 707.
8. Mullards Ltd. (Southampton), private communication, 1976.
9. T. CLAESON, H. L. LUO, T. R. ANANTHARAMAN and M. F. MERRIAM, *Acta Met.* **14** (1966) 285.
10. R. F. MEHL, *J. Amer. Chem. Soc.* **50** (1928) 381.
11. V. G. RIVLIN, R. M. WAGHORNE and G. I. WILLIAMS, *Phil. Mag.* **13** (1966) 1169.
12. A. J. STRAUSS and R. F. BREBRICK, *J. Phys. Chem. Sol.* **31** (1970) 2293.
13. C. J. GILLHAM, to be published.
14. J. S. ABELL, A. G. CROCKER and H. W. KING, *Phil. Mag.* **21** (1970) 207.
15. D. WEAIRE, *J. Phys. C.* **1** (1968) 210.

Received 10 January and accepted 18 February 1977.